Chromo domain proteins in balanced dosage together with boundary elements cooperate in organising the mating-type chromatin in fission yeast

Jenny Alfredsson-Timmins[1], Mayumi Ishida[2], Jun-ichi Nakayama[2] and Pernilla Bjerling[1*]
[1]Uppsala University Dept. of Medical Biochemistry and Microbiology (IMBIM),
Box 582; SE-751 23 Uppsala; Sweden
[2]Laboratory for Chromatin Dynamics, Center for Developmental Biology,
2-2-3 Minatojima-Minamimachi, Chuo-ku,
Kobe, Hogo 650-0047, Japan
[*]Corresponding author:
Tel.: +46 18 471 6652
Fax: +46 18 471 4673
E-mail: Pernilla.Bjerling@imbim.uu.se

Abstract

The chromatin in the cell nucleus has a spatial organisation. For example, in the fission yeast, *Schizosaccharomyces pombe*, transcriptionally repressed heterochromatin is found at the nuclear membrane (NM). The centromeres and the mating-type region localise in the proximity of the spindle pole body (SPB), while the telomeres are found on the opposite side of the nucleus in the proximity of the nucleolus. In a previous study we used the mating-type region as a model to study the driving force behind nuclear organisation. We proposed two mutually exclusive models to explain what determines the localisation of the mating-type region. The first model suggests that solely the amount of heterochromatin in the region affects the localisation, while the other model stipulates that the boundary elements together with heterochromatin formation anchor the mating-type region in the NM in the vicinity of the SPB. Here, we present data that disproves the first model. We found that in a strain expressing tripled amounts of the chromodomain protein Swi6, a structural component of heterochromatin, the mating-type region was delocalised from the proximity of the SPB. A strain deleted of the histone deacetylase *clr3*$^{+}$ also had a delocalised mating-type locus. Interestingly, a strain with a point-mutation in *clr3-735* producing an enzymatically inactive protein in normal amounts showed an intermediate phenotype. Most importantly, we identify the chromodomain proteins, Chp1 and Chp2, as crucial factors for correct subnuclear localisation of the mating-type region. We suggest that boundary elements together with chromodomain proteins in balanced dosage and composition cooperate in organising the mating-type chromatin.

Introduction

In the cell nucleus the DNA is packed into nucleosomes by wrapping the DNA around an octameric complex of histones. The histones are globular proteins with unstructured N-terminal tails protruding from the nucleosomes. These N-terminal tails are subjected to modifications resulting in two main types of chromatin; active euchromatin

where a majority of expressed genes is found, and transcriptionally repressed heterochromatin (Buhler and Moazed, 2007). In the yeast *Schizosaccharomyces pombe* there are three main regions where heterochromatin is formed; the pericentromeric region, the subtelomeric region and in the mating-type region. Initiation of heterochromatin formation in these three different regions are dependent on slightly different mechanisms. Heterochromatin formation in the pericentromeric region is totally dependent on the RNAi machinery, while in the mating-type region there are redundant mechanisms directing heterochromatin formation (Jia et al., 2004). The molecular characteristics of euchromatin and heterochromatin are conserved between fission yeast and humans. Euchromatin has high levels of acetylation of the N-terminal histone tails and histone H3 is methylated on lysine 4 (H3K4Me). In heterochromatin on the other hand, the N-terminal tails of the histones have low acetylation levels and methylation of lysine 9 at histone H3 (H3K9Me) (Buhler and Moazed, 2007). The latter modification is carried out by methyltransferases; SUV39H1 in humans and in *S. pombe* by its homologue, Clr4 (Rea et al., 2000). This H3K9Me modification creates a binding site for a subfamily of chromodomain proteins of which in the fission yeast there are four; Swi6, Chp1, Chp2 and Clr4 (Bannister et al., 2001; Sadaie et al., 2004; Zhang et al., 2008). Swi6 is a structural component of heterochromatin, Chp1 is a part of the RNA Induced Transcriptional Silencing Complex (RITS) and finally, Chp2 has recently been found to be associated with the SHREC complex containing the histone deacetylase (HDAC) Clr3 (Motamedi et al., 2008; Nakayama et al., 2000; Sugiyama et al., 2007; Verdel et al., 2004). Furthermore, the interdependencies of these chromodomain proteins for binding to the different heterochromatic regions were investigated in (Sadaie et al., 2004). When *clr4*$^{+}$ is deleted, the other three chromodomain proteins are detached from the normally silenced regions (Shin et al., 2005). This is expected since in cells lacking Clr4 there is no H3K9Me modification as Clr4 is the sole histone methyltransferase in *S. pombe* acting on H3K9. When *swi6*$^{+}$ is deleted, Chp1 remain bound to the mating-type region and in a strain lacking Chp2, Chp1 and reduced amounts of Swi6 remain bound to the chromatin of this locus (Sadaie et al., 2004).

Different types of chromatin are known to localise to different nuclear compartments as the chromatin has a non-random organisation in the cell nucleus (Sexton et al., 2007). Subnuclear localisation contributes to gene regulation, although the principles on how this is achieved are not straightforward. For example, in the yeast *Saccharomyces cerevisiae* a gene under the control of a crippled silencer tethered to the NM becomes transcriptionally repressed (Andrulis et al., 1998). However, in the same model organism reports claim that genes are moved to the nuclear pores in the NM upon gene activation (Taddei et al., 2006). In fission yeast on the other hand gene clusters induced during nitrogen starvation are found at the proximity of the NM during normal growth conditions. However, when cells are starved for nitrogen, genes in these clusters are induced and the clusters move to a more internal position in the cell nucleus (Alfredsson-Timmins et al., 2009). The localisation of the clusters to the NM is dependent on the HDAC Clr3 with a mechanism that is not solely dependent on the HDAC activity of the Clr3 protein. A point mutation, *clr3-735*, that gives rise to a full-length protein produced in normal amounts but lacking the HDAC activity results in an intermediate phenotype, between a

wild-type strain and a complete knockout of *clr3*$^{+}$. In the fission yeast interphase nucleus the three main heterochromatic regions are also found at the nuclear periphery. The three centromeres localise at the nuclear membrane by attaching to the spindle pole body (SPB), while the telomeres are found in two to four clusters at the NM on the opposite side of the nucleus as compared to the SPB where the nucleolus is found (Funabiki et al., 1993). In addition, in a wild-type strain the mating-type region is positioned in the proximity of the SPB together with the centromeres (Alfredsson-Timmins et al., 2007). The mating-type region consists of three linked loci; *mat1* is expressed and determines the mating-type, P or M, of the cell, and *mat2-P* and *mat3-M* are two silent storage cassettes. The two silent cassettes are separated by an 11 kb silent region called the K-region. Deletion of the K-region results in a strain with two epigenetic states with a transcriptionally repressed or a transcriptionally derepressed mating-type region respectively (Thon and Friis, 1997). Over-expression of Swi6 by using a strain containing three copies of the gene at the endogenous locus, *swi6-333*, results in a more efficient switch to the transcriptional off state (Nakayama et al., 2000). The boundary between transcriptionally repressed heterochromatin and active euchromatin in the mating-type region is established by the *IR-L* and *IR-R* inverted repeats surrounding *mat2-P* and *mat3-M* (Noma et al., 2001; Thon et al., 2002). The boundary function of these inverted repeats requires the binding of TFIIIC to B-boxes in these elements (Noma et al., 2006). By performing live cell analysis using strains with a Green Fluorescent Protein (GFP) tagged mating-type region we demonstrate that the localisation of the mating-type region to the SPB is dependent on the histone methyltransferase, Clr4 (Alfredsson-Timmins et al., 2007). Moreover, in a strain where the two boundary elements *IR-L* and *IR-R* have been deleted the mating-type region is displaced from its position at the proximity of the SPB but remain at the proximity of the NM. In (Alfredsson-Timmins et al., 2007) we suggested two mutually exclusive models to explain these results. The first model propose that the amount of heterochromatin alone determines the localisation of the mating-type region, and all the effects on chromatin organisation detected in the mutant strains we investigated is a cause of reduced amounts of heterochromatin in this region. The second model suggests that the amount of heterochromatin together with other factors acting via the two boundary elements *IR-L* and *IR-R* cooperate in anchoring the mating-type region to the NM in the vicinity of the SPB.

In this study the aim was to distinguish between these two models, as well as investigate whether additional factors are important for the subnuclear organisation of the mating-type chromatin. We find that the mating-type region was severely delocalised in strains lacking either chromodomain protein Chp1 or Chp2. In addition, surprisingly a strain over-expressing Swi6 had a delocalised mating-type region. Moreover, a strain combining a mating-type region lacking the boundary elements, *IR-L* and *IR-R,* with elevated amounts of Swi6 protein produced from the *swi6-333* allele could not rescue the delocalised mating-type region. This was indicative of the boundary elements performing a function of their own in positioning the mating-type region at the SPB. Finally we found that the histone deacetylase Clr3 was necessary for organisation of the mating-type chromatin, partially through the enzymatic activity and partially due to an additional function of Clr3.

Materials and Methods

Strains and Media. All strains used in this study are listed in Table 1. Standard genetic techniques were used for the crossing of strains. Media were prepared as described in (Thon et al., 1999)

Silencing assay. Silencing assays were performed by growing the cells in YEA (yeast extracts with adenine) liquid media until log phase, then 10-fold serial dilutions were spotted on YEA plates and on YE plates (yeast extract with low adenine) and left to incubate for 4 days at 30ºC.

RNA preparation and quantitative Reverse Transcription-PCR (qRT-PCR) analysis. RNA was extracted as described in (Sadaie et al., 2008). The expression from the *ade6*$^+$ reporter gene was monitored by synthesizing cDNA using Superscript III reverse *trans*criptase (Invitrogen) using an oligo(dT) primer then followed by quantitive PCR analysis using qPCR MasterMix Plus for Sybr Green (Eurogentec) using a 7300 Real-Time PCR System (ABI). Primers used were ade6-qRT-Fw: (5'-CAT GGA AAT TGC AGT GAT GGT AGT-3') and ade6-qRT-Rv: (5'-TGA ATG GTC TCA GTT GTA GGA TAA GC-3') for the *mat3*(*Evo*RV)::*ade6*$^+$ locus and act1-RT-Fw: (5'-CGT GCC CCT GAA GCT CTT T-3') and act1-RT-Rv: (5'-CTC ATG AAT ACC GGC GTT TTC -3') for the *act1*$^+$ locus.

Western Blot. Western blot analysis of Swi6 and Chp2 in wild-type and mutant cells as described in (Sadaie et al., 2008).

ChIP. ChIP analysis and antibodies used as described in (Sadaie et al., 2008)

Microscopy. Cells were grown and mounted as described previously (Alfredsson-Timmins et al., 2007). All fluorescence images were captured using Axiovision 4.6 software using a Zeiss AxioCamMr3 camera mounted on a Zeiss Axio Observer Z1 fluorescence microscope equipped with a 63x Plan-Apochromat objective (N.A=1.40). DsRed and CFP fluorochromes were excited using an HXP 120 fluorescence lamp and emission was detected using the following; DsRed using a DsRed BP filter (Zeiss 42) with 1000 ms exposure time and CFP using a BP filter (Zeiss filterset 47) with an exposure time of 350 ms. GFP was excited with the Colibri 470 nm at 100 % power LED and detected using 488nm GFP filter with an exposure time of 150 ms.

Quantitative image analysis. Quantitative image analysis was performed using the Axiovision 4.6 software. The Axiovision 4.6 software measure tool was used to measure (in μm); the distance from the GFP-labelled chromosomal region to the SPB, the shortest distance from the GFP-labelled chromosomal region to the nuclear periphery and the nuclear diameter in all cells investigated. Only cells where the CFP and GFP were in the same focal plane were used for measurements as the CFP-labelled SPB functions as a fixed reference point when measuring in 2D.

Statistical analysis. SigmaStat®3.5 software was used for the statistical analysis described below. For each strain the mean and median distance from the GFP-labelled locus to the SPB were calculated. Subsequently the standard deviation (SD), min and max distances were calculated. The distance data was binned in groups spanning 0.20 μm and then plotted using the histogram tool in the Data Analysis plug-in of Excel. The observed median distance for all strains, compared to the wild-type strain, were tested statistically (Mann-Whitney Rank Sum Test, $P<0.05$).

Furthermore, the nucleus was divided into three concentric zones of equal surface area using the radius as calculated from the mean nuclear diameter for each strain. There was no difference in the mean diameter between the strains, Zone I correspond to a distance of 0 - 0.22 μm, zone II to a distance of 0.23 - 0.51 μm and zone III to a distance of 0.52 - 1.20 μm from the nuclear periphery. The measured distance from the GFP-labelled chromosomal region to the nuclear periphery for each strain was sorted in ascending order. The distance data for each strain was then placed into one of the three groups, representing Zone I, II or III, and the resulting percentage distributions were plotted as histograms using Excel together with the expected random distribution.

Results

Strain construction. A wild-type strain background with; an *ade6*$^+$ gene at the *Eco*RV site located 500 bp downstream of *mat3-M*, a truncated *ade6-DN/N* allele at the endogenous *ade6*$^+$ *l*ocus, *lacO* repeats inserted at the *his2*$^+$ locus 25 kb centromere-distal from the *mat2/3* region, and the Lac Repressor fused to Green Fluorescent Protein (LacR-GFP) expressed from the *his7*$^+$ locus was constructed. The strain also contained Cut12-Cyano Fluorescent Protein (Cut12-CFP) and Pom152-DsRED labelling the SPB and the NM respectively (Alfredsson-Timmins et al., 2007). The *lacO* repeats enables visualisation of the subnuclear localisation of the chromosomal region via binding of the

LacR-GFP in live cells. This strain background was combined with deletions of genes encoding chromodomain proteins; *swi6Δ, chp1Δ* and *chp2Δ* (Thon and Verhein-Hansen, 2000). Moreover, the *swi6-333* allele where three copies of *swi6*$^+$ are expressed from the endogenous *swi6*$^+$ locus was also crossed into the wild-type strain (Nakayama et al., 2000). Furthermore, deletions of the two boundary elements *IR-L* and *IR-R* were crossed into the wild-type strain (Thon et al., 2002). A strain was also constructed combining the deleted boundary elements *IR-LΔ* and *IR-RΔ* with the *swi6-333* allele. Two further strains; one strain where the gene encoding the HDAC *clr3*$^+$ had been deleted, and one containing a point-mutation in *clr3*$^+$, the *clr3-735* allele, resulting in a full-length protein but lacking in enzymatic activity, were also constructed (Bjerling et al., 2002; Grewal et al., 1998; Grewal and Klar, 1996).

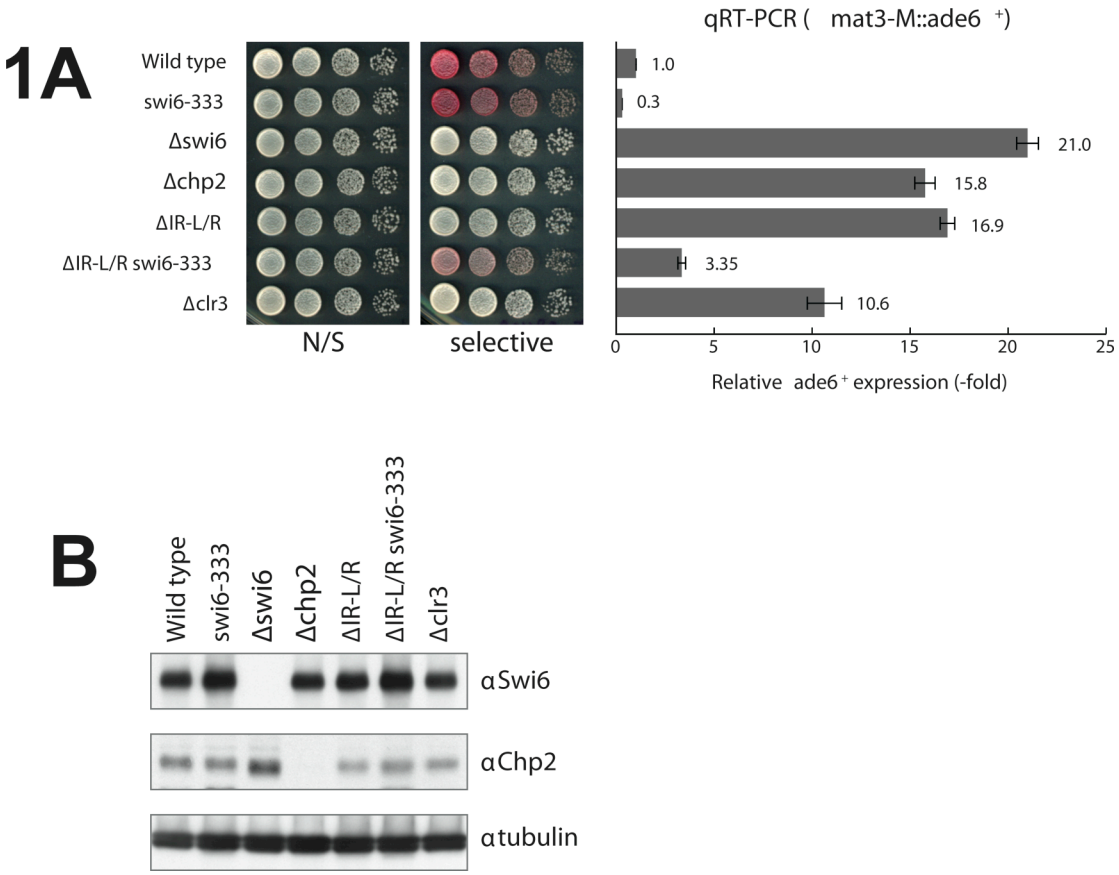

Fig. 1. Effect on the expression of an *ade6*$^+$ reporter gene inserted next to *mat3-M* and cellular abundance of the proteins Swi6 and Chp2 in a wild-type strain and strains carrying *cis*- and *trans*-acting mutations. Strains analysed were; wild type (PJ787), *swi6-333* (PJ836), *swi6Δ* (PJ668), *chp2Δ* (PJ838), *ΔΔ* (PJ579), *ΔΔ swi6-333* (PJ806) and *clr3Δ* (PJ822). (A) Left panel shows silencing assays and the right panel shows RealTime-PCR analysis of the transcriptional levels from the *ade6*$^+$reporter gene at *mat3-M* performed on total RNA from the strains. The numbers to the right of the bars shown the relative ratio of the level of *ade6*$^+$ gene expression in the mating-type region for each strain compared to the wild-type calculated as a ratio between the *ade6*$^+$ reporter gene PCR-product and the *ade6-DN/N* PCR-product. (B) Western blot analysis of the cellular abundance of Swi6 and Chp2 proteins for all strains investigated using antibodies against Swi6 or Chp2. An antibody against tubulin was used as a positive control.

To investigate effects on silencing mediated by these *cis*- and *trans*-acting mutations, the expression from the *ade6*$^+$ reporter gene inserted next to *mat3-M* was monitored by silencing assays and measured using qRT- PCR (Fig. 1A). All the mutant strains contained the truncated allele, *ade6-DN/N*, at the endogenous *ade6*$^+$ locus as an internal control. In the wild-type strain the relative ratio between the *ade6*$^+$ reporter and the *ade6-DN/N* internal control was set to 1.0 (Fig. 1A row 1). The *swi6-333* allele resulted in enhanced silencing of the mating-type region shown as a relative ratio of 0.3 (Fig. 1A row 2). Deletion of the inverted repeats, *IR-L* and *IR-R,* had a strong effect on *ade6*$^+$ *trans*cription resulting in a relative ratio of 16.9 between the reporter gene and the internal control (Thon et al., 2002)(Fig. 1A row 5). Over-expression of Swi6 partially restored the silencing defects in a strain deleted for the boundary elements *IR-L* and *IR-R* to an expression level between the wild-type strain and the strain with the deleted boundary elements (relative ratio of 3.35, Fig. 1A row 6). Silencing mutations in *swi6*$^+$ and *chp2*$^+$ caused a derepression of the reporter gene, relative ratios 21.0 and 15.8 respectively, consistent with previous reports. Finally, *clr3Δ* caused derepression of the reporter gene with a relative ratio of 10.6 (Bjerling et al., 2002; Ekwall and Ruusala, 1994; Freeman-Cook et al., 2005; Thon and Verhein-Hansen, 2000)(Fig. 1A rows 3, 4 and 7).

Interdependencies of the silencing factors in the association with the mating-type region

To confirm the expression of Swi6 and Chp2 proteins, Western blot analysis was performed using antibodies against Swi6 or Chp2 for all strains investigated, and an antibody against tubulin was used as a positive control (Fig. 1B). There was an increase in the amount of Swi6 in both the *swi6-333* and *IR-LΔ IR-RΔ swi6-333* strains (Fig. 1B column 2 and 6). In the *swi6Δ* strain there was a slight increase in the amount of Chp2 (Fig. 1B column 3). Next, we wanted to investigate whether the association of the chromodomain proteins Swi6 and Chp2 with the mating-type region was affected in the various mutated strains. To this end, Chromatin Immunoprecipitations (ChIP) assays were performed where DNA was purified from anti-Swi6 and anti-Chp2 immunoprecipitates from wild-type and strains containing *cis*- and *trans*-acting mutations. The precipitated DNA was PCR amplified using primers against the *ade6*$^+$ gene. The expression signal from *mat3-M*::*ade6*$^+$ relative to the endogenous *ade6-DN/N* in the ChIP result was normalised to the whole-cell extract (WCE) signal and the relative fold enrichment was calculated.

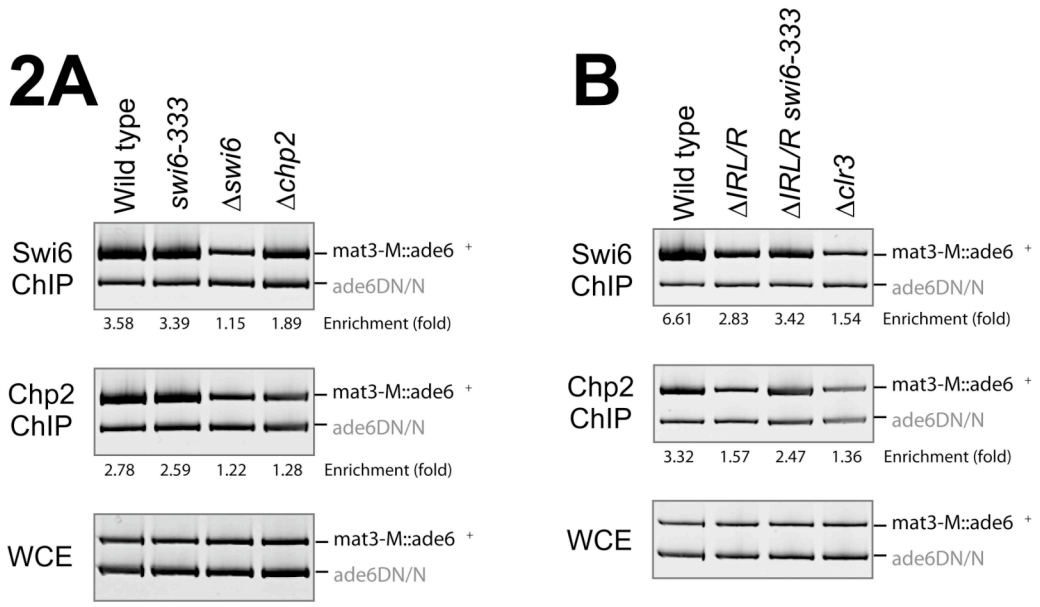

Fig. 2. ChIP assays of the association of Swi6 and Chp2 with the *ade6*$^+$ reporter gene inserted at the mating-type locus performed on purified DNA from anti-Swi6 and anti-Chp2 immunoprecipitates from wild-type and mutant stains carrying *cis*- and *trans*- acting mutations. The purified DNA was PCR amplified and the expression signal from *mat3-M*::*ade6*$^+$ relative to the endogenous *ade6DN/N* in the ChIP result was normalised to the whole-cell extract (WCE) signal and the relative fold enrichment is shown beneath each lane. Strains analysed were; (A) wild-type (PJ787), *swi6-333* (PJ836), *swi6Δ* (PJ668) and *chp2Δ* (PJ838) (B) wild-type (PJ787), *ΔΔ* (PJ579), *ΔΔ swi6-333* (PJ806) and *clr3Δ* (PJ822).

Over expressing Swi6 did not have an effect on the Swi6 binding to the reporter gene (Fig. 2A top panel row 2). Furthermore, in the same strain there was no effect on Chp2 binding (Fig. 2A middle panel row 2). In the *swi6Δ* strain, as expected there was no specific enrichment of Swi6, and there was a decrease in the binding of Chp2 to the *ade6*$^+$ reporter gene consistent with previous results (Fig. 2A top and middle panels row 3)(Sadaie et al., 2004). As expected, there was a reduction in the amount of Chp2 in the *chp2Δ* strain and there was also a slight decrease in Swi6 association with the mating-type region (Fig. 2A top and middle panels row 4). The decrease in Swi6 binding was different from previous findings that actually reported an increase (Sadaie et al., 2004). This discrepancy might be explained by the fact that a different part of the mating-type region was investigated in the previous study. Consistent with a previous report the amount of Swi6 associated with the mating-type region in a *clr3Δ* strain background was reduced (Yamada et al., 2005)(Fig. 2B top and middle panels row 1 and 4 respectively). In addition, a reduction of the Chp2 was also evident in the *clr3Δ* strain background (Fig. 2B middle panel row 4). In the strain with deleted boundary elements there were reduced amounts of Swi6 bound to the reporter gene inserted into the mating-type region and over-expressing Swi6 only slightly compensates for the reduced amounts of bound protein (Fig. 2B top panel row 2 and 3). Moreover, in the *IR-LΔ IR-RΔ* strain background there was also a decrease in mating-type associated Chp2 (Fig. 2B middle panel row 2). From these results we conclude that we detect strong interdependencies between *cis*- and *trans*- acting silencing factors in the association with the mating-type region.

Table 1. List of *S. pombe* strains used in this study.

Strain	Genotype	Source
PJ787	*h⁹⁰ mat3-M(EcoRV)::ade6⁺ his7⁺::dis1placI-GFP his2⁻ [::ura4⁺ kanMX6 lacO] pom152-DsRed::hphMX6 cut12-CFP::natMX6 ura4-D18 leu1-32 ade6-DN/N*	This study
PJ909	*h⁹⁰ mat3-M(EcoRV)::ade6⁺ chp1Δ::LEU2⁺ his7⁺::dis1placI-GFP his2⁻ [::ura4⁺ kanMX6 lacO] pom152-DsRed::hphMX6 cut12-CFP::natMX6 ura4-D18 leu1-32 ade6-DN/N*	This study
PJ838	*h⁹⁰ mat3-M(EcoRV)::ade6⁺ chp2Δ::LEU2⁺ his7⁺::dis1placI-GFP his2⁻ [::ura4⁺ kanMX6 lacO] pom152-DsRed::hphMX6 cut12-CFP::natMX6 ura4-D18 leu1-32 ade6-DN/N*	This study
PJ668	*h⁹⁰ mat3-M(EcoRV)::ade6⁺ swi6Δ::ura4⁺ his7⁺::dis1placI-GFP his2⁻ [::ura4⁺ kanMX6 lacO] pom152-DsRed::hphMX6 cut12-CFP::natMX6 ura4-D18 leu1-32 ade6-DN/N*	Alfredsson-Timmins 2007
PJ836	*h⁹⁰ mat3-M(EcoRV)::ade6⁺ swi6-333::LEU2⁺ his7⁺::dis1placI-GFP his2⁻ [::ura4⁺ kanMX6 lacO] pom152-DsRed::hphMX6 cut12-CFP::natMX6 ura4-D18 leu1-32 ade6-DN/N*	This study
PJ579	*h⁹⁰ mat3-M(EcoRV)::ade6⁺ IR-LΔ/IR-RΔ his7⁺::dis1placI-GFP his2⁻ [::ura4⁺ kanMX6 lacO] pom152-DsRed::hphMX6 cut12-CFP::kanMX6 ura4-D18 leu1-32 ade6-DN/N*	Alfredsson-Timmins 2007
PJ806	*h⁹⁰ mat3-M(EcoRV)::ade6⁺ IR-LΔ/IR-RΔ swi6-333::LEU2⁺ his7⁺::dis1placI-GFP his2⁻ [::ura4⁺ kanMX6 lacO] pom152-DsRed::hphMX6 cut12-CFP::natMX6 ura4-D18 leu1-32 ade6-DN/N*	This study
PJ822	*h⁹⁰ mat3-M(EcoRV)::ade6⁺ clr3Δ::kanMX6 his7⁺::dis1placI-GFP his2⁻ [::ura4⁺ kanMX6 lacO] pom152-DsRed::hphMX6 cut12-CFP::natMX6 ura4-D18 leu1-32 ade6-DN/N*	This study
PJ927	*h⁹⁰ mat3-M(EcoRV)::ade6⁺ clr3-735 his7⁺::dis1placI-GFP his2⁻ [::ura4⁺ kanMX6 lacO] pom152-DsRed::hphMX6 cut12-CFP::kanMX6 ura4-D18 leu1-32 ade6-DN/N*	This study

Chromodomain proteins Swi6, Chp1 and Chp2 are all necessary for the localisation of the mating-type region.

The subnuclear localisation of the mating-type region was investigated by live cell analysis of cells using a fluorescence microscope. In the wild-type strain the mating-type region was found in the proximity of the SPB close to the NM (Fig. 3A panel 1). The median distance between the mating-type region and the SPB was 0.46 μm and between the mating-type region and the NM it was 0.32 μm (Table 2 and 3). The distance between the SPB and the mating-type region was slightly longer in this study as compared to earlier findings presumably due to the use of different microscope techniques. The previous study was performed using confocal microscopy and there the median distance between the mating-type region and the SPB was 0.29 μm (Alfredsson-Timmins et al., 2007). The median distance between the mating-type region and NM are very similar using different microscopy techniques, here 0.32 μm, and 0.34 μm in (Alfredsson-Timmins et al., 2007) (Table 2). Furthermore, the mean diameter of 2.4 μm of the cell nucleus was determined by using the Pom152-DsRed signal. The mean diameter was used to divide the cell nucleus into

three concentric zones of equal surface area. Zone I is the nuclear periphery, defined as 0-0.22 μm from the NM, zone II is next to the nuclear periphery, found between 0.23-0.51 μm from the NM and finally 0.52-1.20 μm is zone III, the nuclear interior. In a wild-type strain the mating-type region was predominantly found in zone II, next to the nuclear periphery (Fig. 3A panel 1).

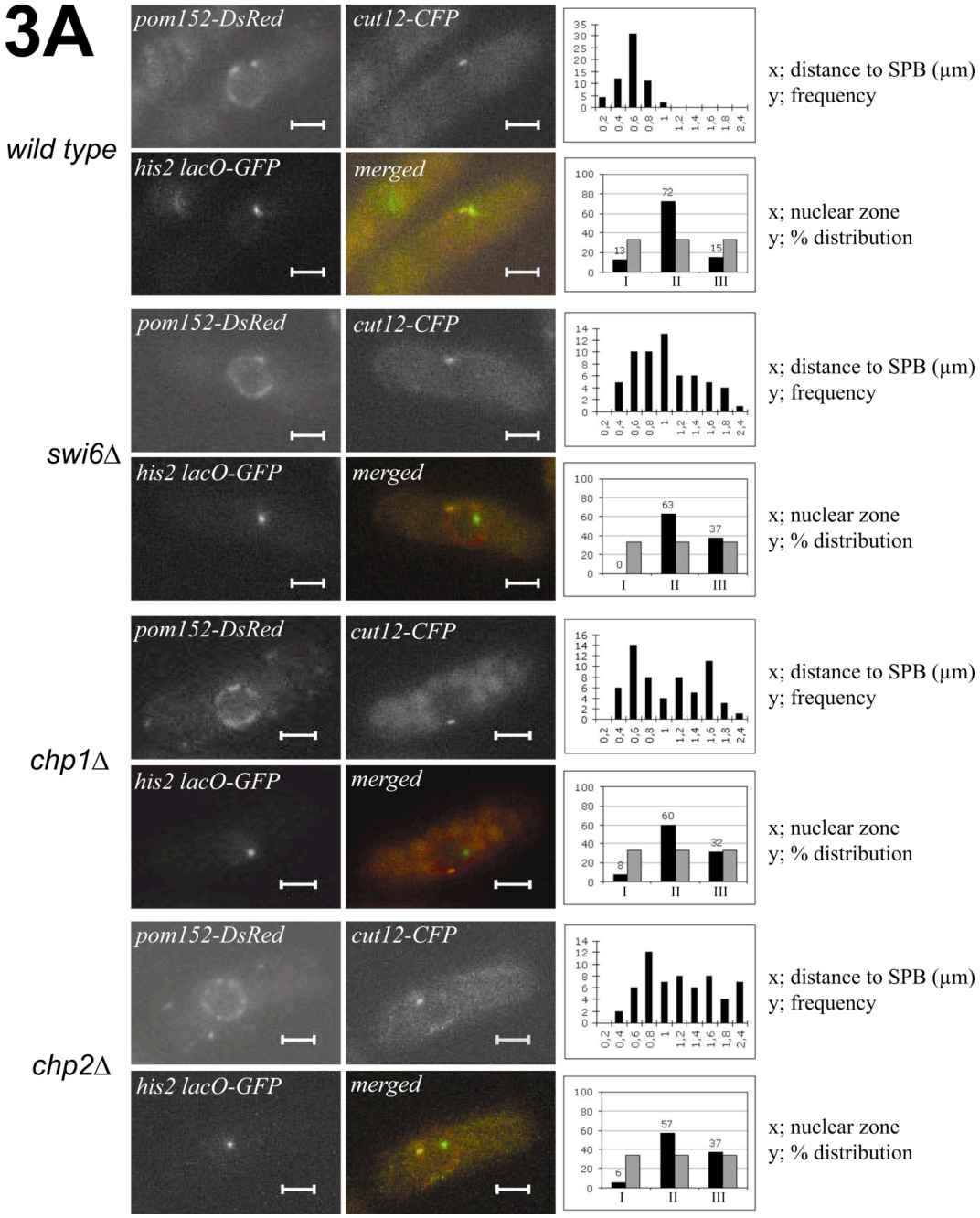

Fig. 3A. The mating-type region was localised close to the SPB at the nuclear periphery in the wild-type strains and was delocalised in strains with *cis*- and *trans*- acting mutations. Fluorescence microscopy images of wild-type and mutant cells. In the different panels are; the nuclear membrane labelled with DsRed (top left), the SPB component Cut12 labelled with CFP (top middle), the mating type region labelled with lacR-GFP (bottom left) and merged images (bottom middle). The scale bars in all Figures correspond to 2 μm. Histograms with the distributions of observed distances between the GFP and CFP signals binned in groups spanning 0.2 μm (top right). The nucleus was divided into three zones of equal surface area, and the observed distribution of *mat2/3* localisation into zone I, zone II or zone III for each strain was plotted. Zone I correspond to a distance of 0 - 0.22 μm, zone II to a distance of 0.23 - 0.51μm and zone III to a distance of 0.52 - 1.20 μm from the nuclear periphery (bottom right). The strains analysed were; wild type (PJ787), *chp1Δ* (PJ909), *swi6Δ* (PJ668) and *chp2Δ* (PJ838).

Previously we have shown that Swi6 is important for positioning the mating-type region at the SPB, and this was confirmed in Fig. 3A panel 2, and Table 2 and 3. Next, we wanted to investigate the importance of other chromodomain proteins on the subnuclear localisation of the mating-type region. Chp1 is a component of the RNA induced transcriptional silencing complex (RITS) which is important in initiating and maintaining transcriptional silencing of the centromeres in *S. pombe*, but not the mating-type region (Sadaie et al., 2004; Thon and Verhein-Hansen, 2000; Verdel et al., 2004). We used a strain lacking Chp1 to investigate whether this chromodomain protein also has a role in correct positioning of the mating-type region. Since *chp1Δ* does not have any silencing defects in the mating-type region it was an unexpected finding that deleting Chp1 result in a delocalised *mat2/3* region. In the *chp1Δ* strain there was a shift in the zone occupancy from zone II to zone II with 60% of the cells localising to zone II and 32 % to zone III (Fig. 3A panel 3). There was also an increase both in the distance to the SPB, from 0.46 μm to 0.82 μm, and to the NM from 0.32 μm to 0.42 μm. Both these changes were statistically significant (P<0.05)(Table 2 and 3). We then continued to investigate the localisation of the mating-type region in a *chp2Δ* strain background (Sadaie et al., 2004; Shin et al., 2005). In this mutant strain background the mating-type region was severely delocalised (Fig. 3A panel 4). The delocalisation with respect to the SPB was even greater in a *chp2Δ* mutant background as compared to the *swi6Δ* background, with a distance of 1.07 μm between the SPB and the mating-type region in the strain with a deletion of *chp2*$^{+}$ as compared to the distance of 0.83 μm in the strain lacking Swi6 protein (Table 2). This was unexpected since there was just a reduction of Swi6 binding to the mating-type region in the *chp2Δ* background (Fig. 2A top panel row 4). This difference in localisation of the mating-type region between the two strains with chromodomain deletions was significant (P<0.05)(Tables 2 and 3). We conclude that the chromodomain proteins Swi6, Chp1 and Chp2 were all important for the localisation of the mating-type region.

Table 2. Descriptive statistics of the distances between the *lacO*-GFP locus and the SPB

Strain	n	Mean (μm)	Median (μm)	S.D.	Min value (μm)	Max value (μm)	Different from wild type (P<0.05)
wild type	60	0.48	0.46	0.169	0.14	0.97	n.a.
chp1Δ	60	0.95	0.82	0.47	0.23	1.89	yes
chp2Δ	60	1.11	1.07	0.480	0.29	2.07	yes
swi6Δ	60	0.94	0.83	0.427	0.27	1.98	yes
swi6-333	60	0.58	0.54	0.221	0.2	1.11	yes
IR-LΔ IR-RΔ	60	0.99	1.01	0.404	0.32	1.79	yes
IR-LΔ/IR-RΔ swi6-333	60	0.90	0.87	0.382	0.31	1.74	yes
clr3Δ	60	1.10	1.03	0.445	0.33	1.96	yes
clr3-735	60	0.84	0.77	0.434	0.23	1.88	yes

n.a. not applicable

Enhanced silencing does not correlate with localisation to the nuclear periphery.

To investigate if over-expressing the chromodomain protein Swi6 had an effect on localisation of the *mat2/3* region, a strain carrying the *swi6-333* allele, which expresses three times the normal amount of Swi6, was analysed. In this strain with enhanced silencing, the mating-type region was unexpectedly found at a more interior position as compared to the wild-type situation (Fig. 1A row 2 and Fig. 3B panel 1). The median distance between the SPB and the mating-type region increased from 0.46 μm to 0.54 μm and the distance between the mating-type region and the NM increased from 0.32 μm to 0.42 μm (Table 2 and 3). Both these changes are significant (P<0.05). We conclude that there is no strict correlation between enhanced silencing, heterochromatin formation and localisation to the nuclear periphery.

Table 3. Descriptive statistics of the distances between the *lacO*-GFP locus and the NM

Strain	n	Mean (μm)	Median (μm)	s.d.	Min value (μm)	Max value (μm)	Different from wild type (P<0.05)
wild type	60	0.35	0.32	0.136	0.14	0.72	n.a.
chp1Δ	60	0.47	0.42	0.23	0.14	1.13	yes
chp2Δ	60	0.48	0.43	0.206	0.14	0.97	yes
swi6Δ	60	0.50	0.42	0.205	0.23	1.02	yes
swi6-333	60	0.43	0.42	0.182	0.14	0.92	yes
IR-LΔ IR-RΔ	60	0.44	0.41	0.214	0.14	0.94	yes
IR-LΔ IR-RΔ swi6-333	60	0.50	0.51	0.193	0.20	1.13	yes
clr3Δ	60	0.48	0.46	0.211	0.14	1.11	yes
clr3-735	60	0.44	0.37	0.205	0.20	1.05	yes

n.a. not applicable

Boundary elements have a function of their own in positioning the mating-type region.

When the boundary elements *IR-L* and *IR-R* were deleted the mating-type region was delocalised from the SPB, but remain in the proximity of the NM, as has previously been reported (Alfredsson-Timmins et al., 2007)(Fig. 3B panel 2). We previously found that in the strain where the boundary elements are deleted the mating-type region localise 0.41 μm from the NM compared to a distance of 0.34 μm of the wild-type strain. This is not significantly different (P<0.05) (Alfredsson-Timmins et al., 2007). In this study using another microscopy technique, we measure the same distance of 0.41 μm from the NM for the mating-type region lacking the boundary elements, however this value was significantly different from the distance of 0.32 μm between the wild-type mating-type region and the NM (P<0.05)(Table 2 and 3). The differences obtained in the statistical tests from the two studies was due to the shorter distances in the wild-type strain between the mating-type region and the NM and lesser spread of the values in the current study, and these might be explained by the different microscope techniques used.

Moreover, when viewing the data as occupancy in the different zones of the cell nucleus a large portion of the cells still have the mating-type region in zone II (58 %)(Fig. 3B panel 2). We conclude that the mating-type region lacking the boundary elements was delocalised both from the SPB and NM, but predominantly stay in zone II, next to the nuclear periphery.

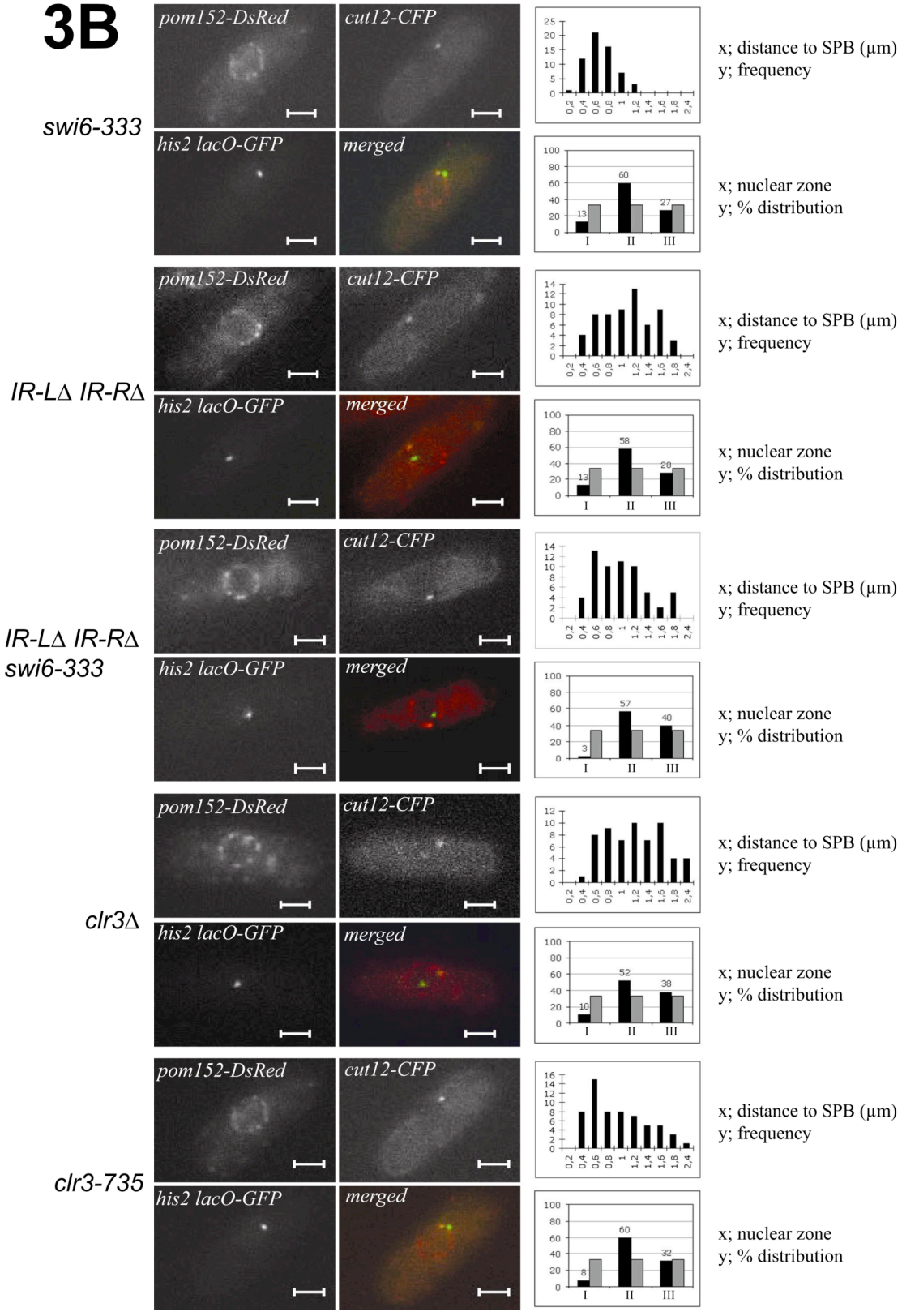

Fig. 3B. The mating-type region was localised close to the SPB at the nuclear periphery in the wild-type strains and was delocalised in strains with *cis-* and *trans-* acting mutations. Fluorescence microscopy images of wild-type and mutant cells. In the different panels are; the nuclear membrane labelled with DsRed (top left), the SPB component Cut12 labelled with CFP (top middle), the mating type region labelled with lacR-GFP (bottom left) and merged images (bottom middle). The scale bars in all Figures correspond to 2 μm. Histograms with the distributions of observed distances between the GFP and CFP signals binned in groups spanning 0.2 μm (top right). The nucleus was divided into three zones of equal surface area, and the observed distribution of *mat2/3* localisation into zone I, zone II or zone III for each strain was plotted. Zone I correspond to a distance of 0 - 0.22 μm, zone II to a distance of 0.23 - 0.51μm and zone III to a distance of 0.52 - 1.20 μm from the nuclear periphery (bottom right). The strains analysed were; *swi6-333* (PJ836), *ΔΔ* (PJ579), *ΔΔ swi6-333* (PJ806), *clr3Δ* (PJ822) and *clr3-735* (PJ927).

Next we tried to compensate for the reduced amounts of heterochromatin found in the mating-type region in an *IR-LΔ IR-RΔ* strain background by combing the deletions with the *swi6-333* allele. The effects on silencing indicate that we have partially compensated for the heterochromatin loss in an *IR-LΔ IR-RΔ* strain by introducing a *swi6-333* allele since the relative ratio between the reporter gene and the internal control was reduced to 3.35 from 16.9 (Fig. 1A rows 5 and 6). The increased amount of Swi6 did not restore the defect in localisation of the mating-type region caused by the deleted boundary elements (Fig. 3B panel 3). The decrease in distance to the SPB from 1.01 μm in *IR-LΔ IR-RΔ* strain to 0.87 μm in the *IR-LΔ IR-RΔ swi6-333* strain is not significantly different (P<0.05) (Table 2). Comparing the distance from the mating-type region to the NM between the *IR-LΔ IR-RΔ* strain background and the *IR-LΔ IR-RΔ swi6-333* strain, there is an increase from 0.41 μm in the strain deleted for the boundary elements to 0.51 μm in the strain with the deleted boundary elements over-expressing Swi6 (Table 3). We conclude that the boundary elements have a function of their own and the delocalisation of the mating-type region detected in the *IR-LΔ IR-RΔ* deletion mutant does not merely reflect a decrease in the amount of heterochromatin in the region.

The histone modifying enzyme Clr3 has a role in localisation of the mating-type region.

In (Alfredsson-Timmins et al., 2007) we showed that the Clr4 methyltransferase is important for the localisation of the mating-type region. In this study we wanted to investigate whether the histone deacetylase Clr3 was also important for subnuclear localisation of the mating-type region. Clr3 is known to be important for heterochromatin formation as cells lacking this enzyme have elevated acetylation levels of the histones in the mating-type region (Bjerling et al., 2002). When *clr3*$^+$ was deleted the *mat2/3* region was displaced both from the SPB and the NM. The distance to the SPB and NM increased to 1.03 μm and 0.46 μm respectively. Moreover, in the *clr3Δ* strain 52% of the cells were found in zone II and 38% in zone three (Fig. 3B panel 4 and Table 2 and 3). When introducing a point-mutation in the *clr3*$^+$ gene, the c*lr3-735* allele, it results in a full-length protein although it lacks its enzymatic activity (Grewal et al., 1998; Grewal and Klar, 1996). The mating-type region was delocalised also in the *clr3-735* strain (Fig. 3B panel 5). The distance to the SPB is 0.77 μm and 0.37 μm to the NM (Table 2 and 3). The majority of cells were still found in zone II and zone III as for the *clr3Δ* but in the *clr3-735* strain there was a slight dominance of zone II occupancy as compared to the strain completely

lacking Clr3. This means that the point-mutation has a less severe delocalisation phenotype as compared to the *clr3Δ* strain showing an intermediate phenotype between the wild-type strain and the *clr3Δ* mutant strain. From these results we conclude that apart from its enzymatic activity the chromatin modifier Clr3 also has another role in positioning the mating-type region correctly in the interphase nucleus.

Discussion

All chromodomain proteins binding to H3K9Me were necessary for the localisation of the mating-type region at the SPB

In a wild-type strain the GFP tagged mating-type region was found in the vicinity of the SPB, predominantly in zone II, next to the nuclear periphery (Fig. 3A panel 1). Previously we have shown that the chromodomain protein Swi6 is necessary for the organisation of the mating-type chromatin (Alfredsson-Timmins et al., 2007). In this study we found that the chromodomain proteins Chp1 and Chp2 were also crucial for the positioning of the mating-type region in the cell nucleus. The delocalised mating-type region in a *chp1Δ* strain was surprising since Chp1 is not necessary for heterochromatin formation in the mating-type region. There are additional mechanisms independent of RNAi that recruits silencing factors to the mating-type region (Jia et al., 2004). Moreover, also the strong delocalization phenotype in *chp2Δ* was surprising. In a strain lacking Chp2 the mating-type region was even more delocalised as compared to a strain lacking Swi6 (Fig. 3A panel 2 and 3). This was an unexpected result since in a *chp2Δ* strain background previous reports have shown that Swi6 and Chp1 are still bound to the K-region in the middle of the silent mating-type region (Sadaie et al., 2004). Here we detect reduced amounts of Swi6 bound to the *ade6*$^{+}$ reporter gene inserted in the centromere distal part of the mating-type region (Fig. 2A top panel row 4). Although, a modification characteristic of active chromatin, namely H3MeK4, increases in a strain lacking Chp2, the H3K9Me modification level is still high (Sadaie et al., 2004; Shin et al., 2005). Moreover, in the *chp2Δ* mutant background reporter genes inserted into the normally silent area are expressed, but the mating-type cassettes themselves remain silent (Thon and Verhein-Hansen, 2000). This is not the case in a *clr4Δ* strain where the *mat2-P* and *mat3-M* cassettes are also derepressed (Thon et al., 1994), indicating a less severe silencing defect in the *chp2Δ* mutant background as compared to for example the *clr4Δ* mutant strain. The results for the *chp2Δ* strain can also be due to Chp2 having a more structural role in attaching the mating-type region to the NM, possibly via its chromoshadow domain. In (Sadaie et al., 2008) they find that in fractionation assays Chp2 is associated with the pellet, an indication of a possible nuclear membrane interaction. Furthermore, in the same study fractionation assays from strains expressing chimeric chromodomain proteins they find that both the hinge and chromoshadow domains of Chp2 are indispensable for the pellet association.

Enhanced silencing in the nuclear interior with dispersed silencing factors

When a *swi6-333* allele, was introduced into the wild-type strain, resulting in three times more Swi6 protein, the mating-type region was shifted to a more internal position, seen as an increase in the observed distance between the mating-type region and

the SPB. In addition, more cells were scored as having their mating-type region in the nuclear interior (Fig. 3B panel 1). In a wild-type strain the Swi6 protein has a distinct localisation pattern, forming two to five discrete spots representing the centromeres, telomeres and the mating-type region (Ekwall et al., 1995). Enhanced silencing of the mating-type region in the *swi6-333* strain even though it is detached from its normal position in the proximity of the SPB could be explained if over expression of Swi6 causes a diffusion of the protein throughout the nucleus. Using antibodies against Swi6 we detected a more diffuse staining pattern of Swi6 in a *swi6-333* strain as compared to a wild-type strain indicating availability of Swi6 throughout the nucleus (data not shown). In *Saccharomyces cerevisiae* the subtelomeric regions are transcriptionally silenced by a complex of Sir proteins and attach to the nuclear membrane via Ku anchor, and when Ku is deleted, Sir proteins are found throughout the nucleus (Taddei et al., 2009). In this situation with repressor proteins throughout the nucleus, silencing of a reporter gene occurs in the nuclear interior. This silencing occurs provided that the reporter gene is next to a strong *cis*-acting silencing element capable of recruiting Sir proteins (Taddei et al., 2009).

The boundary elements have a function of their own in organising the mating-type chromatin

In (Alfredsson-Timmins et al., 2007) we proposed two mutually excusive models of what determines the localisation of the mating-type region in the cell nucleus. The first model suggests that it is only the amount of heterochromatin that determines the localisation of the mating-type region. The more heterochromatin, the closer the mating-type region is to the SPB. In this model the effects on organisation of the mating-type chromatin, when the boundary elements *IR-L* and *IR-R* are deleted, would be due to reduced amounts of heterochromatin in the mating-type region in this mutant strain (Alfredsson-Timmins et al., 2007; Thon et al., 2002). The second model suggests that the boundary elements *IR-L* and *IR-R* anchor the mating-type region to the NM next to the SPB in a Clr4 dependent manner. Our results here clearly disprove the first model since over-expression of Swi6, with enhanced silencing, resulted in a more internal localisation of the mating-type region (Fig. 3B panel 1). Moreover, by expressing three times the normal amount of Swi6 the delocalisation effects of the mating-type region when the two boundary elements *IR-L* and *IR-R* are deleted could not be rescued (Fig. 3B panel 3). On the contrary, tripled Swi6 expression resulted in more cells where the mating-type region was in the nuclear interior as compared to the strain background with deleted boundary elements and wild-type levels of Swi6 protein (Fig. 1B row 5 and Fig. 3B panel 2). These results indicate that the boundary elements have a function of their own in positioning of the mating-type region in the cell nucleus.

HDAC Clr3 was necessary for the correct localisation of the mating-type region

In a previous report we found that a strain lacking the histone methyltransferase Clr4 had a delocalised mating-type region (Alfredsson-Timmins JCS 2007). We wanted to investigate whether the HDAC Clr3 might also have a role in subnuclear positioning of the mating-type region. In strains lacking the enzyme Clr3, the mating-type region was delocalised from both the SPB and the NM (Fig. 3B panel 4). In this and in a previous study we showed that

deleting *clr3*$^{+}$ cause a more severe delocalisation phenotype than by just introducing a point-mutation in the *clr3*$^{+}$ gene, the *clr3-735* allele, which produces a full length protein only lacking in its enzymatic activity. This indicates the Clr3 also has structural role (Alfredsson-Timmins et al., 2009) (Fig. 3B panel 4 and 5). Interestingly Chp2 associates with the Clr3 containing SHREC complex (Motamedi et al., 2008) leading to the speculation that perhaps Chp2 helps positioning the mating-type chromatin at the NM via binding of its chromoshadow domain to Clr3. Moreover, in mammalian cells LAP2β interacts with HDAC3 at the nuclear envelope resulting in transcriptional repression (Somech et al., 2005).

In conclusion we propose that the boundary elements together with critical amounts and correct composition of the chromodomain proteins Swi6, Chp1 and Chp2 are necessary for correct positioning of the mating-type region in the vicinity of the SPB next to the NM in *S. pombe,* and that possibly an interaction between Chp2 and Clr3 is important for attachment of this region to the NM.

Acknowledgements

We thank Geneviève Thon and Shiv Grewal for sending us strains. This work was supported by grant 2004-3286 from the Swedish Research Council.

References

Alfredsson-Timmins, J., Henningson, F. and Bjerling, P. (2007). The Clr4 methyltransferase determines the subnuclear localization of the mating-type region in fission yeast. ***J Cell Sci* 120, 1935-43.**

Alfredsson-Timmins, J., Kristell, C., Henningson, F., Lyckman, S. and Bjerling, P. (2009). Reorganization of chromatin is an early response to nitrogen starvation in Schizosaccharomyces pombe. ***Chromosoma* 118, 99-112.**

Andrulis, E. D., Neiman, A. M., Zappulla, D. C. and Sternglanz, R. (1998). Perinuclear localization of chromatin facilitates transcriptional silencing. ***Nature* 394, 592-5.**

Bannister, A. J., Zegerman, P., Partridge, J. F., Miska, E. A., Thomas, J. O., Allshire, R. C. and Kouzarides, T. (2001). Selective recognition of methylated lysine 9 on histone H3 by the HP1 chromo domain. ***Nature* 410, 120-4.**

Bjerling, P., Silverstein, R. A., Thon, G., Caudy, A., Grewal, S. and Ekwall, K. (2002). Functional divergence between histone deacetylases in fission yeast by distinct cellular localization and in vivo specificity. ***Mol Cell Biol* 22, 2170-81.**

Buhler, M. and Moazed, D. (2007). **Transcription and RNAi in heterochromatic gene silencing. *Nat Struct Mol Biol* 14, 1041-1048.**

Ekwall, K., Javerzat, J. P., Lorentz, A., Schmidt, H., Cranston, G. and Allshire, R. (1995). The chromodomain protein Swi6: a key component at fission yeast centromeres. ***Science* 269, 1429-31.**

Ekwall, K. and Ruusala, T. (1994). Mutations in rik1, clr2, clr3 and clr4 genes asymmetrically derepress the silent mating-type loci in fission yeast. ***Genetics* 136, 53-64.**

Freeman-Cook, L. L., Gomez, E. B., Spedale, E. J., Marlett, J., Forsburg, S. L., Pillus, L. and Laurenson, P. (2005). Conserved locus-specific silencing functions of Schizosaccharomyces pombe sir2+. ***Genetics* 169, 1243-60.**

Funabiki, H., Hagan, I., Uzawa, S. and Yanagida, M. (1993). Cell cycle-dependent specific positioning and clustering of centromeres and telomeres in fission yeast. *J Cell Biol* 121, 961-76.

Grewal, S. I., Bonaduce, M. J. and Klar, A. J. (1998). Histone deacetylase homologs regulate epigenetic inheritance of transcriptional silencing and chromosome segregation in fission yeast. ***Genetics* 150, 563-76.**

Grewal, S. I. and Klar, A. J. (1996). Chromosomal inheritance of epigenetic states in fission yeast during mitosis and meiosis. ***Cell* 86, 95-101.**

Jia, S., Noma, K. and Grewal, S. I. (2004). RNAi-independent heterochromatin nucleation by the stress-activated ATF/CREB family proteins. ***Science* 304, 1971-6.**

Motamedi, M. R., Hong, E. J., Li, X., Gerber, S., Denison, C., Gygi, S. and Moazed, D. (2008). HP1 proteins form distinct complexes and mediate heterochromatic gene silencing by nonoverlapping mechanisms. ***Mol Cell* 32, 778-90.**

Nakayama, J., Klar, A. J. and Grewal, S. I. (2000). A chromodomain protein, Swi6, performs imprinting functions in fission yeast during mitosis and meiosis. ***Cell* 101, 307-17.**

Noma, K., Allis, C. D. and Grewal, S. I. (2001). Transitions in distinct histone H3 methylation patterns at the heterochromatin domain boundaries. ***Science* 293, 1150-5.**

Noma, K., Cam, H. P., Maraia, R. J. and Grewal, S. I. (2006). A Role for TFIIIC Transcription Factor Complex in Genome Organization. ***Cell* 125, 859-72.**

Rea, S., Eisenhaber, F., O'Carroll, D., Strahl, B. D., Sun, Z. W., Schmid, M., Opravil, S., Mechtler, K., Ponting, C. P., Allis, C. D. et al. (2000). Regulation of chromatin structure by site-specific histone H3 methyltransferases. ***Nature* 406, 593-9.**

Sadaie, M., Iida, T., Urano, T. and Nakayama, J. (2004). A chromodomain protein, Chp1, is required for the establishment of heterochromatin in fission yeast. *Embo J* 23, 3825-35.

Sadaie, M., Kawaguchi, R., Ohtani, Y., Arisaka, F., Tanaka, K., Shirahige, K. and Nakayama, J. (2008). Balance between distinct HP1 family proteins controls heterochromatin assembly in fission yeast. ***Mol Cell Biol* 28, 6973-88.**

Sexton, T., Schober, H., Fraser, P. and Gasser, S. M. (2007). Gene regulation through nuclear organization. ***Nat Struct Mol Biol* 14, 1049-1055.**

Shin, J. A., Choi, E. S., Kim, H. S., Ho, J. C., Watts, F. Z., Park, S. D. and Jang, Y. K. (2005). SUMO modification is involved in the maintenance of heterochromatin stability in fission yeast. ***Mol Cell* 19, 817-28.**

Somech, R., Shaklai, S., Geller, O., Amariglio, N., Simon, A. J., Rechavi, G. and Gal-Yam, E. N. (2005). The nuclear-envelope protein and transcriptional repressor LAP2beta interacts with HDAC3 at the nuclear periphery, and induces histone H4 deacetylation. *J Cell Sci* 118, 4017-25.

Sugiyama, T., Cam, H. P., Sugiyama, R., Noma, K., Zofall, M., Kobayashi, R. and Grewal, S. I. (2007). SHREC, an effector complex for heterochromatic transcriptional silencing. ***Cell* 128, 491-504.**

Taddei, A., Van Houwe, G., Hediger, F., Kalck, V., Cubizolles, F., Schober, H. and Gasser, S. M. (2006). Nuclear pore association confers optimal expression levels for an inducible yeast gene. ***Nature* 441, 774-8.**

Taddei, A., Van Houwe, G., Nagai, S., Erb, I., van Nimwegen, E. and Gasser, S. M. (2009). The functional importance of telomere clustering: global changes in gene expression result from SIR factor dispersion. ***Genome Res* 19, 611-25.**

Thon, G., Bjerling, K. P. and Nielsen, I. S. (1999). Localization and properties of a silencing element near the mat3-M mating-type cassette of Schizosaccharomyces pombe. ***Genetics* 151, 945-63.**

Thon, G., Bjerling, P., Bunner, C. M. and Verhein-Hansen, J. (2002). Expression-state boundaries in the mating-type region of fission yeast**. *Genetics* 161, 611-22.**

Thon, G., Cohen, A. and Klar, A. J. (1994). Three additional linkage groups that repress transcription and meiotic recombination in the mating-type region of Schizosaccharomyces pombe. ***Genetics* 138, 29-38.**

Thon, G. and Friis, T. (1997). Epigenetic inheritance of transcriptional silencing and switching competence in fission yeast. ***Genetics* 145, 685-96.**

Thon, G. and Verhein-Hansen, J. (2000). Four chromo-domain proteins of Schizosaccharomyces pombe differentially repress transcription at various chromosomal locations. ***Genetics* 155, 551-68.**

Verdel, A., Jia, S., Gerber, S., Sugiyama, T., Gygi, S., Grewal, S. I. and Moazed, D. (2004). RNAi-mediated targeting of heterochromatin by the RITS complex. ***Science* 303, 672-6.**

Yamada, T., Fischle, W., Sugiyama, T., Allis, C. D. and Grewal, S. I. (2005). The nucleation and maintenance of heterochromatin by a histone deacetylase in fission yeast. *Mol Cell* **20, 173-85.**

Zhang, K., Mosch, K., Fischle, W. and Grewal, S. I. (2008). Roles of the Clr4 methyltransferase complex in nucleation, spreading and maintenance of heterochromatin. *Nat Struct Mol Biol* 15, 381-8.

Table S1. The nucleus was divided into three zones of equal surface area using the mean diameter for all strains for calculations. Zone I corresponds to a distance of 0 - 0.22 μm, zone II 0.23 - 0.51μm and zone III.52 - 1.20 μm from the NM. In all cells used for measurements the observed distance was determined as the distance from the lacO-GFP locus to the NM. The observed distance data was ten placed into zone I, II or III. All strains investigated were tested using χ^2 -test statistics to determine if the observed distribution was different from that of a random distribution

Strain	n	zone I	zone II	zone III	Different from random (p-value)
wild type	60	8	43	9	yes (2.39472×10^{-9})
chp1Δ	60	5	36	19	yes (1.49367×10^{-9})
chp2Δ	60	4	34	22	yes (1.11955×10^{-5})
swi6Δ	60	0	38	22	yes (1.24693×10^{-8})
swi6-333	60	8	36	16	yes (3.04325×10^{-5})
IR-LΔ IR-RΔ	60	8	35	17	yes (7.86896×10^{-5})
IR-LΔ IR-RΔ swi6-333	60	2	34	24	yes (1.51514×10^{-6})
clr3Δ	60	6	31	23	yes (2.88735×10^{-4})
clr3-735	60	5	36	19	yes (1.49367×10^{-9})